

Valley polarization due to trigonal warping on tunneling electrons in graphene

This article has been downloaded from IOPscience. Please scroll down to see the full text article.

2009 J. Phys.: Condens. Matter 21 045301

(<http://iopscience.iop.org/0953-8984/21/4/045301>)

View [the table of contents for this issue](#), or go to the [journal homepage](#) for more

Download details:

IP Address: 129.252.86.83

The article was downloaded on 29/05/2010 at 17:28

Please note that [terms and conditions apply](#).

Valley polarization due to trigonal warping on tunneling electrons in graphene

J M Pereira Jr¹, F M Peeters^{2,3}, R N Costa Filho^{3,4} and G A Farias³

¹ Instituto de Física, Universidade Federal de Alagoas, Maceió, Alagoas 57072-970, Brazil

² Department of Physics, University of Antwerp, Groenenborgerlaan 171, B-2020 Antwerpen, Belgium

³ Departamento de Física, Universidade Federal do Ceará, Fortaleza, Ceará 60455-760, Brazil

⁴ Department of Physics, University of Western Ontario, London, ON, N6A 3K7, Canada

Received 4 July 2008, in final form 18 November 2008

Published 19 December 2008

Online at stacks.iop.org/JPhysCM/21/045301

Abstract

The effect of trigonal warping on the transmission of electrons tunneling through potential barriers in graphene is investigated. We present calculations of the transmission coefficient for single and double barriers as a function of energy, incidence angle and barrier heights. The results show remarkable valley-dependent directional effects for barriers oriented parallel to the armchair or parallel to the zigzag direction. These results indicate that electrostatic gates can be used as valley filters in graphene-based devices.

(Some figures in this article are in colour only in the electronic version)

1. Introduction

Monolayers of crystalline carbon (graphene) have been intensively studied in recent years (for a review see, e.g., [1]). That interest was spurred by the development of techniques for the production of graphene [2–4], together with the observation of striking electronic and mechanical properties in these systems. Many of the unusual properties of graphene arise from the gapless and approximately linear dispersion of charge carriers at two inequivalent points (the K and K' valleys) in the vicinity of the Fermi energy. Energy gaps can arise in narrow graphene ribbons [5], or by the coupling with impurities [6] or with a substrate [7]. This control of the spectrum, together with a large room-temperature carrier mobility, is expected to lead to the creation of carbon-based nanoelectronic devices [8, 9].

The linear spectrum of carriers in graphene allows one to describe the dynamics of the charge carriers in single layers of graphene as that of massless fermions, with a 'light speed' equal to the Fermi velocity of the crystal. In this description, the valley states, which can be seen as internal degrees of freedom of the carriers, are independent and degenerate. Theoretical work has shown that the valley degeneracy can be lifted by the introduction of short range perturbations such as defects, as well as by the influence of the edges of the graphene sample.

There have been proposals to develop structures that can selectively act on these valley states, in order to create 'valleytronic' devices [10], in analogy with spintronic

applications. Most proposals require the use of valley-selective interaction of carriers with the edges of graphene point contacts. In parallel to that, it has been shown that the tunneling of charge carriers through potential barriers in graphene can be quite distinct from that of a conventional 2D electron gas. In particular, the transmission coefficient displays a strong angular dependence for both barriers and wells, with the barrier becoming completely transparent at normal incidence (Klein paradox) [11–13, 15]. A recent paper [14] investigated the propagation of electrons through quantum structures in graphene including the effect of trigonal warping (TW). This effect is a modification of the conical dispersion of the carriers as the energy scale increases, due to the symmetry of the crystal lattice. In their calculation, the authors assumed that the transmission coefficient would not be significantly affected by the inclusion of TW and considered only the dependence of the carrier group velocity on the potential. In this work we show that this assumption does not hold in general, and that the transmission probability can in fact be substantially modified by TW. The results show that the inclusion of TW introduces an anisotropy in the transmission that is valley-dependent and thus can be used as an alternative way of creating a valley-polarized current in graphene.

The energy of the carriers in single-layer graphene can be obtained from a tight-binding model that, in the presence of a potential U , can be expressed as

$$E = \pm \hbar v_F \sqrt{k^2(1 - 3sk_x a/2) + 2sk_x^3 a + k^4 a^2/16} + U, \quad (1)$$

where $s = 1(-1)$ for electrons in the K (K') valley, v_F is the Fermi velocity in graphene ($\approx 1 \times 10^6$ m s⁻¹), $k = \sqrt{k_x^2 + k_y^2}$ is the wavevector and a is the lattice parameter of the crystal ($a \approx 0.142$ nm). The k_x (k_y) component of the momentum corresponds to propagation along the armchair (zigzag) direction in the lattice (see figure 1(a)). In the following calculations we assumed a defect-free graphene sheet of infinite extension. Thus, we do not incorporate any valley scattering effect.

2. Model

In order to obtain numerical results for the transmission probability as a function of energy and momentum $T(E, k)$ we considered square potential barriers and imposed the continuity of the wavefunction solutions at the barrier interfaces. For the double barrier case, each potential barrier was assumed to have heights U_a and U_b , and widths L_a and L_b , separated by a distance W (see figure 1(b)). For the single barrier case we set $U_b = 0$. The calculation of the transmission coefficient is similar to the one described in [11], except that in the present case, due to the TW effect, the results for large potentials become sensitive not only to the direction of the electron momentum with respect to the potential barrier but also with respect to the lattice. We consider two cases, namely (a) barriers aligned parallel to the x axis, which corresponds to the armchair side of the lattice (see figure 1(c)) and barriers parallel to the y axis, which corresponds to the zigzag side of the lattice (figure 1(d)).

2.1. The zigzag case

Let us first consider the case of barriers aligned parallel to the y axis. In this case, the solutions inside and outside the barrier are matched along the zigzag direction of the lattice. One then has to find k_x by solving the equation

$$\frac{a^2}{16}k_x^4 + \left(\frac{as}{2}\right)k_x^3 + \left(1 + \frac{a^2}{8}k_y^2\right)k_x^2 - \left(\frac{3}{2}ask_y^2\right)k_x + \left[k_y^2 + \frac{a^2}{16}k_y^4 - (\epsilon - u)^2\right] = 0. \quad (2)$$

A convenient way of solving the above equation is by an iterative method, starting with

$$k_{x,0}^2 = (\epsilon - u)^2 - k_y^2 - \frac{a^2}{16}k_y^4 \quad (3)$$

and then using

$$k_{x,n+1}^2 = \left[(\epsilon - u)^2 - k_y^2 - \frac{a^2}{16}k_y^4\right] + \left(\frac{3}{2}ask_y^2\right)k_{x,n} - \left(\frac{a^2}{8}k_y^2\right)k_{x,n}^2 - \left(\frac{as}{2}\right)k_{x,n}^3 - \frac{a^2}{16}k_{x,n}^4. \quad (4)$$

A brief inspection of equation (4) shows that, for a given energy, the values of k_x are expected to differ depending on s . However, equation (4) indicates that the transmission should be expected to be invariant under a transformation of the momentum component parallel to the barrier, $k_y \rightarrow -k_y$. It must be emphasized that, in the ballistic regime, the

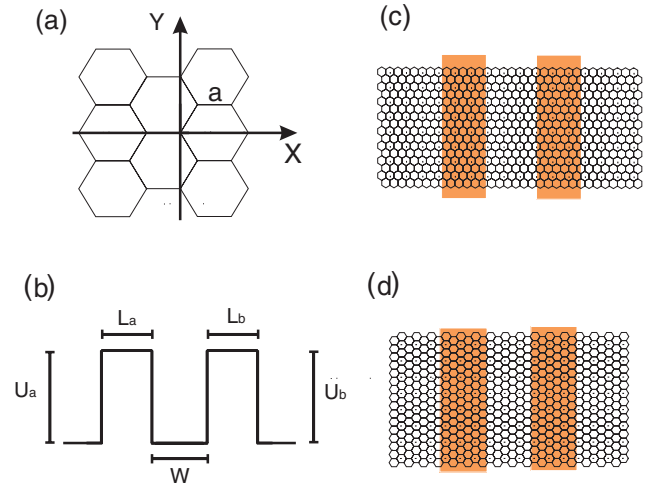


Figure 1. Schematic depiction of the double barrier system. (a) Potential orientation and orientation of the lattice and (b) potential parameters. (c) Barriers along the armchair and (d) zigzag orientation.

transmission through a potential barrier is critically dependent on the values of the normal component of the wavevector (i.e. k_x in this case) at each point, and also on whether this wavevector component is real or imaginary. Therefore, the valley asymmetry in the transmission must not depend qualitatively on the particular shape of the potential barrier interfaces, although it is expected to arise only for large values of the barrier height.

2.2. The armchair case

Let us now consider potential barriers aligned parallel to the x axis, which is along the armchair side of the lattice.

By solving equation (1) for the y component of the wavevector one obtains

$$k_y = \pm \left[-\frac{8}{a^2} \left(1 - \frac{3ask_x}{2}\right) - k_x^2 \pm \frac{8}{a^2} \sqrt{\left(1 - \frac{3ask_x}{2}\right)^2 - \frac{k_x^3 a^3 s}{2} + \frac{a^2}{4}(\epsilon - u)^2} \right]^{1/2}, \quad (5)$$

where $\epsilon = E/\hbar v_F$ and $u = U/\hbar v_F$. By taking the internal sign as positive and expanding the internal square root, the above expression can be approximated for small values of $k_x a$ as

$$k_y = \pm \sqrt{\frac{(\epsilon - u)^2}{\left(1 - \frac{3ask_x}{2}\right)} - k_x^2}. \quad (6)$$

Thus, for $a \rightarrow 0$, it gives $k_y = \pm \sqrt{(\epsilon - u)^2 - k_x^2}$. These expressions show that the TW creates an anisotropy of the dispersion, given that the value of k_y is sensitive to the sign of k_x . It should be noticed that, in equation (5), a change of sign for the valley label s is equivalent to a change of sign of the momentum component parallel to the barrier interface (k_x , in this case). Therefore, this anisotropy should be present in transmission properties of electrons in potential barriers.

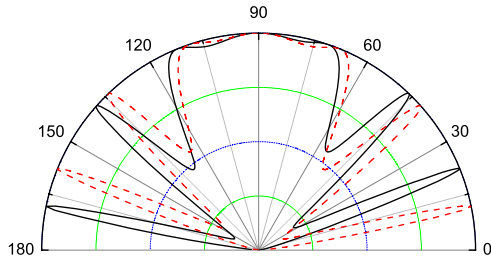


Figure 2. Incidence angle dependence of the transmission coefficient for a single barrier in the armchair orientation, for carriers associated with K (solid black lines) and K' (red dashed lines) valleys. Parameters given in the text.

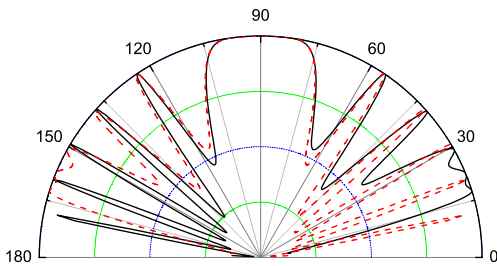


Figure 3. The same as figure 2 but now for a double barrier.

3. Results

3.1. The armchair case

As seen from equation (5), for the armchair case the value of k_y is sensitive to the sign of k_x . A striking consequence of that anisotropy is an asymmetry in the angular dependence of the transmission, as shown in figure 2. The figure shows the transmission coefficient for carriers with $E = 50$ meV, interacting with a square barrier of $U_b = 200$ meV and $L = 500$ nm. The solid line shows the results for $s = 1$ (i.e. K valley), whereas the dashed line corresponds to $s = -1$ (K' valley). The results show that the asymmetry of the transmission becomes conspicuous for large incidence angles, with the appearance of transmission peaks at different angles for each valley label. Using a double barrier structure, this valley filtering effect is enhanced for slanted incidence of the electrons. This is shown in figure 3 where the transmission is shown as a function of incidence angle ($T(\theta)$) for a double barrier with $U_a = U_b = 300$ meV, $L_a = L_b = 50$ nm and $W = 25$ nm for carriers with $E = 54$ meV.

3.2. The zigzag case

For barriers aligned parallel to the y axis (zigzag orientation), the asymmetry in the transmission occurs between incoming electrons (i.e. moving 'to the right', with positive k_x) and outgoing (moving 'to the left', with negative k_x) electrons. The situation is reversed in each valley. Therefore, the large potential steps created in p-n junctions at a armchair orientation in graphene can create a valley-polarized current by means of a valley-selective transmission. Figure 4 shows results for a double barrier with $U_a = U_b = 200$ meV and

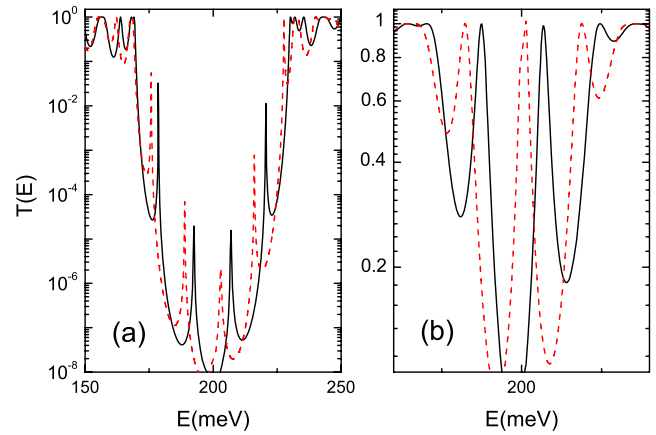


Figure 4. Transmission coefficient as a function of energy for a double barrier along the zigzag orientation for carriers associated with K (black solid line) and K' (red dashed line) valleys for (a) $k_x = 0.05$ nm⁻¹ and (b) $k_x = 0.01$ nm⁻¹.

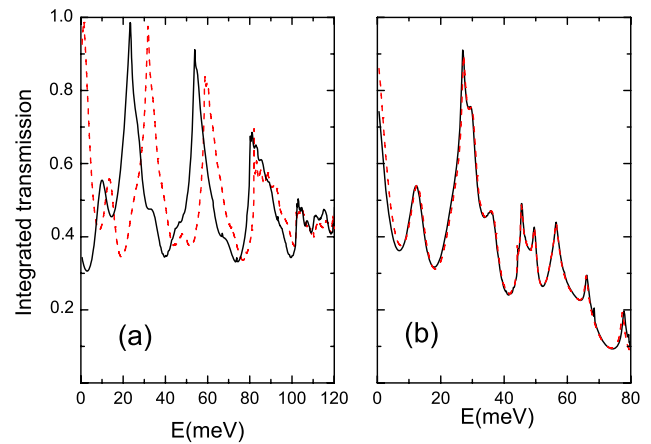


Figure 5. Integrated transmission as a function of energy for a double barrier in the zigzag orientation for carriers of K (black solid line) and K' (red dashed line) valleys for (a) $U_a = U_b = 300$ meV and (b) $U_a = U_b = 100$ meV.

$L_a = L_b = W = 100$ nm where (a) $k_y = 0.05$ nm⁻¹ and (b) $k_y = 0.01$ nm⁻¹. The black solid line corresponds to incoming (outgoing) and the red dashed line to outgoing (incoming) carriers of the K (K') valley.

The previous results for the transmission were calculated for a fixed value of the y component of the momentum and figure 4 indicates that the position and distribution of the transmission peaks are momentum-dependent. In an experiment, the relevant energy is the Fermi energy and the transmission should be averaged over the Fermi surface. Figure 5 shows results for the transmission integrated over all incidence angles as a function of energy. These results were calculated for two sets of double barriers with $L_a = L_b = 50$ nm and $W = 100$ nm with (a) $U_a = U_b = 300$ meV and (b) $U_a = U_b = 100$ meV. The results in figure 5 show that the valley asymmetry is strongly dependent on the barrier height, becoming negligible for lower barriers. Figure 6 shows a valley polarization factor, which was obtained from the ratio between the integrated transmission probability for each valley

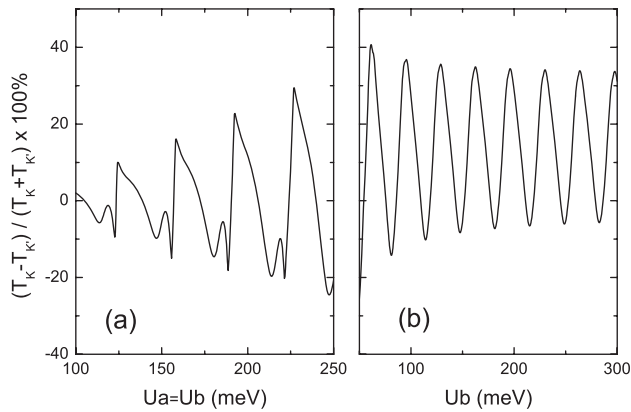


Figure 6. Valley polarization calculated from the integrated transmission for each valley as a function of barrier height for double barriers in the zigzag orientation for (a) $U_a = U_b$ and (b) $U_a = 300$ meV.

(i.e. $T_K - T_{K'}$) and the total transmission (i.e. $T_K + T_{K'}$). In this case we took $E = 20$ meV and the results are shown as a function of the barrier heights for two cases, namely (a) $U_a = U_b$ and (b) $U_a = 300$ meV. In both cases $L_a = L_b = 50$ nm and $W = 100$ nm. As can be seen, the degree of polarization oscillates as the potential barriers are raised, with the valley asymmetry becoming larger as the barrier heights increase. The asymmetry was observed in the zigzag configuration for single as well as double barriers, where the valley-selective behavior was enhanced by resonance effects. Additionally, when one barrier is kept fixed, the difference in transmission for each valley oscillates, which raises the prospect of the design of a tunable valley filter device. This asymmetry in the integrated transmission does not arise in the armchair case, since in that case $T_K(E, \theta) = T_{K'}(E, \pi - \theta)$ as shown in figures 2 and 3.

4. Conclusions

In summary, we demonstrated a valley-selective effect for the transmission of carriers in graphene-based quantum structures. The effect is a consequence of the valley asymmetry induced by the trigonal warping of the carrier dispersion. It can be enhanced by the use of multiple barriers and can be exploited for the development of future valleytronic devices. We showed the effect for square barriers but the results are also valid

for rounded barriers and the determining factor is the height of the potential barriers and the orientation of the barriers with respect to the lattice. Therefore, in the absence of intervalley scattering, a system of two barriers in which the first acts as a ‘polarizer’ and the second as an ‘analyzer’ allows the use of the valley degree of freedom as an additional means of controlling the current in graphene-based devices. Alternatively, one could employ potential barriers coupled to graphene nanoribbons with zigzag edges. These are known to support valley-polarized currents and a constriction on such ribbons has also been proposed as valley filters [10]. The valley polarization itself can be detected in graphene in contact with superconductor electrodes [16].

Acknowledgments

This work was supported by the Brazilian Council for Research (CNPq), the Flemish Science Foundation (FWO-VI), the Belgian Science Policy (IUAP) and the Flemish–Brazilian collaborative program.

References

- [1] Castro Neto A H, Guinea F, Peres N M R, Novoselov K S and Geim A K 2007 arXiv:0709.1163v1[cond-mat]
- [2] Novoselov K S *et al* 2004 *Science* **306** 666
- [3] Novoselov K S *et al* 2005 *Nature* **438** 197
- [4] Zhang Y, Tan Y W, Stormer H L and Kim P 2005 *Nature* **438** 201
- [5] Han M Y, Özyilmaz B, Zhang Y and Kim P 2007 *Phys. Rev. Lett.* **98** 206805
- [6] Costa Filho R N, Farias G A and Peeters F M 2007 *Phys. Rev. B* **76** 193409
- [7] Zhou S Y *et al* 2007 *Nat. Mater.* **6** 770
- [8] Liang X, Fu Z and Chou S Y 2007 *Nano Lett.* **7** 3840
- [9] Liang G *et al* 2007 *J. Appl. Phys.* **102** 054307
- [10] Rycerz A, Tworzydło J and Beenakker C W J 2007 *Nat. Phys.* **3** 172
- [11] Katsnelson M I, Novoselov K S and Geim A K 2006 *Nat. Phys.* **2** 620
- [12] Cheianov V V and Fal’ko V I 2006 *Phys. Rev. B* **74** 041403
- [13] Pereira J M Jr, Mlinar V, Peeters F M and Vasilopoulos P 2006 *Phys. Rev. B* **74** 045424
- [14] Garcia-Pomar J L, Cortijo A and Nieto-Vesperinas M 2007 arXiv:0710.1004v1[cond-mat]
- [15] Pereira J M Jr, Vasilopoulos P and Peeters F M 2007 *Appl. Phys. Lett.* **90** 132122
- [16] Akhmerov A R and Beenakker C W J 2007 *Phys. Rev. Lett.* **98** 157003